

Adiabatic connection interaction strength interpolation method made accurate for the uniform electron gas

Lucian A. Constantin,¹ Subrata Jana,² Szymon Śmiga,³ and Fabio Della Sala^{4,1}

¹*Institute for Microelectronics and Microsystems (CNR-IMM),
Via Monteroni, Campus Unisalento, 73100 Lecce, Italy*

²*Department of Molecular Chemistry and Materials Science,
Weizmann Institute of Science, Rehovoth 76100, Israel*

³*Institute of Physics, Faculty of Physics, Astronomy and Informatics,*

Nicolaus Copernicus University in Toruń, ul. Grudziądzka 5, 87-100 Toruń, Poland

⁴*Center for Biomolecular Nanotechnologies, Istituto Italiano di Tecnologia, Via Barsanti 14, 73010 Arnesano (LE), Italy*

(Dated: September 29, 2023)

The adiabatic connection interaction strength interpolation (ISI)-like method provides a high-level expression for the correlation energy, being in principle exact in the weak-interaction limit, where it recovers the second-order Görling-Levy perturbation term, but also in the strong-interaction limit that is described by the strictly correlated electron approach. In this work, we construct the genISI functional made accurate for the uniform electron gas, a solid-state physics paradigm that is a very difficult test for ISI-like correlation functionals. We assess the genISI functional for various jellium spheres with the number of electrons $Z \leq 912$ and for the non-relativistic noble atoms with $Z \leq 290$. For the jellium clusters, the genISI is remarkably accurate, while for the noble atoms, it shows a good performance, similar to other ISI-like methods. Then, the genISI functional can open the path using the ISI-like method in solid-state calculations.

I. INTRODUCTION

The Density Functional Theory (DFT)^{1,2}, is exact in principle, but in practice, the exchange-correlation (XC) energy $E_{xc}[n(\mathbf{r})]$ as a functional of the electronic density $n(\mathbf{r})$ must be approximated. The XC functional should contain all the many-body quantum effects raised by the electron-electron interactions beyond the Hartree method. Nowadays, there are known important exact properties of $E_{xc}[n]$ that have been used in the construction of many XC functional approximations, that are classified on the so-called Jacob's ladder^{3,4}. The first rung of the ladder is the Local Density Approximation (LDA)^{2,5,6} which has been constructed from the uniform electron gas (UEG) model system⁷. The UEG is one of the most important model systems for the XC functional development, being a solid-state paradigm. In fact, LDA is still often used in solid-state calculations because of its remarkable accuracy for various properties, such as surface energy of transition metals⁸ and work function^{9,10}.

One of the most rigorous paths for constructing new XC functionals is via the adiabatic connection (AC) method¹¹⁻¹⁷, that gives the exact XC energy as the following coupling-constant integral

$$E_{xc}[n] = \int_0^1 d\alpha W_{xc,\alpha}[n], \quad (1)$$

where

$$W_{xc,\alpha}[n] = \langle \Psi_n^{min,\alpha} | \hat{V}_{ee} | \Psi_n^{min,\alpha} \rangle - U[n]. \quad (2)$$

Here $U[n] = (1/2) \int d\mathbf{r} \int d\mathbf{r}' n(\mathbf{r})n(\mathbf{r}')/|\mathbf{r} - \mathbf{r}'|$ is the Hartree energy, \hat{V}_{ee} is the Coulomb repulsion operator, and $\Psi_n^{min,\alpha}$ is the antisymmetric wave function that yields the density $n(\mathbf{r})$ and minimizes the expectation

value $\langle \hat{T} + \alpha \hat{V}_{ee} \rangle$, with \hat{T} being the kinetic energy operator, and $\alpha \geq 0$ the coupling constant (known also as interaction strength). We note that $\Psi_n^{min,\alpha=1} = \Psi_n^{min}$ is the interacting, exact ground-state wavefunction for density $n(\mathbf{r})$ and $\Psi_n^{min,\alpha=0} = \Phi_n^{min}$ is the non-interacting KS wavefunction for density $n(\mathbf{r})$ given in the form of Slater determinant. Considering that the exchange energy functional is, by definition,

$$E_x[n(\mathbf{r})] = \langle \Phi_n^{min}(\mathbf{r}) | \hat{V}_{ee} | \Phi_n^{min}(\mathbf{r}) \rangle - U[n(\mathbf{r})],$$

then the adiabatic connection integrand $W_{xc,\alpha}[n]$ can be also written as

$$\begin{aligned} W_{xc,\alpha}[n] &= E_x[n] + W_{c,\alpha}[n], \\ W_{c,\alpha}[n] &= \langle \Psi_n^{min,\alpha} | \hat{V}_{ee} | \Psi_n^{min,\alpha} \rangle - \langle \Phi_n^{min} | \hat{V}_{ee} | \Phi_n^{min} \rangle. \end{aligned} \quad (3)$$

The AC was often used in the construction of accurate hybrid functionals^{16,18-21}, and especially the most sophisticated, fifth-rung functionals, including the Görling-Levy (GL) perturbation correlation terms²²⁻²⁴, the random phase approximation (RPA), and RPA-like methods based on XC kernel approximations²⁵⁻³⁸.

In this work, we will focus on the high-level interaction strength interpolation (ISI) methods³⁹⁻⁴⁴, that accurately interpolate between the weak- ($\alpha \rightarrow 0$) and strong- ($\alpha \rightarrow \infty$) interaction limits. Such methods have been intensively studied and tested⁴⁵⁻⁶⁶. Efficient implementation of ISI methods are also available in public quantum-chemistry codes⁶⁷.

In the weak-interaction limit, the GL perturbation theory becomes exact, and $W_{xc,\alpha}[n]$ is^{23,39,68}

$$W_{xc,\alpha \rightarrow 0}[n] = W_0[n] + W_0'[n]\alpha + \dots + W_0^{(m)}[n]\alpha^m + \dots, \quad (4)$$

where $W_0[n] = E_x[n]$ is the exact DFT exchange functional, $W'_0[n] = 2E_c^{GL2}[n]$, and $W_0^{(m)}[n] = (m + 1)E_c^{GL_{m+1}}[n]$. In this work, as in most of the ISI-like methods, we consider only the first two terms of the perturbation expansion.

On the other hand, in the strong-interaction limit, $W_{xc,\alpha}[n]$ behaves as⁴⁴

$$W_{xc,\alpha \rightarrow \infty}[n] = W_\infty[n] + W'_\infty[n]\alpha^{-1/2} + W_\infty^{(2)}[n]\alpha^{-3/2} + \dots, \quad (5)$$

where $W_\infty[n]$, $W'_\infty[n]$ can be in principle exactly calculated using the strictly correlated electron (SCE) approach^{69–71}. In practice, generalized gradient approximation (GGA) models have been developed for $W_\infty[n]$ and $W'_\infty[n]$ ^{40,60,62}.

Eq. (5) shows that the α^{-1} -term in the expansion should be zero. However, the original ISI method³⁹ has a spurious α^{-1} -term, that was removed in the revISI⁴³ and LB⁴⁴ methods.

The total XC energy of ISI methods can be expressed as

$$E_{xc}[n] = \mathcal{F}(E_x, E_c^{GL2}, W_\infty, W'_\infty) \quad (6)$$

where \mathcal{F} is a non-linear function of the ingredients E_x and E_c^{GL2} and of the density functionals W_∞ and W'_∞ . Eq. 6 thus resembles (also from a computational cost point-of-view) the one of double-hybrid (DH) functionals⁷²: however, the former employs a non-linear dependence from the GL2 (or MP2) term and do not diverges for systems with vanishing gaps^{52,63,67}, which is a clear superiority with respect to DH approaches.

However, the ISI methods have difficulties to recover the logarithmic singularity of the UEG correlation energy per particle in the high-density limit ($\epsilon_c \propto \ln(r_s)$ when $r_s \rightarrow 0$, where r_s is the bulk parameter), but all of them are accurate in the UEG low-density limit (at $r_s \rightarrow \infty$)^{40,73}. We recall that the high-density limit of the UEG correlation energy is exactly described by the RPA method⁶.

In spite of this limitation, we construct an ISI-like method, named genISI, that is very accurate for the UEG correlation energy when $r_s \geq 1$. Note that most materials are characterized by $1 \leq r_s \leq 10$. Thus, one could expect increased accuracy of the proposed method.

The paper is organized as follows. In section II, we present the construction of genISI XC functional. Computational details are described in Section III, while in section IV, we report the correlation energies results of genISI and other ISI-like methods for the UEG model system, various jellium clusters, non-relativistic noble atoms and small systems for which the exact quantities (W'_0 , W_∞ , W'_∞) are known exactly. Finally, in section V, we summarize our conclusions.

II. THE GENISI XC FUNCTIONAL

We start the construction of genISI XC functional considering the UEG limit (denoted by UEG-ISI), where $W'_0 \rightarrow -\infty$ and $W'_0/W_0 \rightarrow \infty$. In fact, in the UEG, the energy-gap vanishes and thus the GL2 correlation diverges.

A. The UEG-ISI XC functional

Let us consider the revISI expression⁴³ for the UEG-ISI XC functional

$$W_{xc,\alpha}^{UEG-ISI}[n] = W_\infty[n] + \frac{b(2 + c\alpha + 2d\sqrt{1 + c\alpha})}{2\sqrt{1 + c\alpha}(d + \sqrt{1 + c\alpha})^2}, \quad (7)$$

so that the UEG-ISI XC energy is

$$\begin{aligned} E_{xc}^{UEG-ISI}[n] &= \int_0^1 d\alpha W_{xc,\alpha}^{UEG-ISI}[n] \\ &= W_\infty[n] + \frac{b[n]}{d + \sqrt{1 + c[n]}} \end{aligned} \quad (8)$$

In Ref. 43 the parameters b , c , d were functions of W'_0 , which tends to $-\infty$ for the UEG. Here, instead, we define:

$$\begin{aligned} b[n] &= (W_0 - W_\infty)(1 + d), \\ c[n] &= b[n]^2 / [4W_\infty'^2]. \end{aligned} \quad (9)$$

The functionals $b[n]$ and $c[n]$ have been found such that $W_{xc,\alpha}^{UEG-ISI}[n]$ has the following properties:

$$\begin{aligned} W_{xc,\alpha \rightarrow 0}^{UEG-ISI}[n] &\longrightarrow W_0 - \frac{(W_0 - W_\infty)^3(1 + d)}{4W_\infty'^2} \alpha + \mathcal{O}(\alpha^2), \\ W_{xc,\alpha \rightarrow \infty}^{UEG-ISI}[n] &\longrightarrow W_\infty + W'_\infty \alpha^{-1/2} + \mathcal{O}(\alpha^{-3/2}). \end{aligned} \quad (10)$$

Then, $W_{xc,\alpha}^{UEG-ISI}[n]$ recovers the strong interaction limit of Eq. (5), and the first leading term of the weak interaction limit expansion of Eq. (4). Of course, the first perturbation term $W'_0[n]\alpha$ can not be fulfilled by $W_{xc,\alpha}^{UEG-ISI}[n]$, because in the UEG limit $W'_0 = -\infty$, such that $W_{xc,\alpha}^{UEG-ISI}[n]$ should be a function only of W_0 , W_∞ , and W'_∞ .

We also mention that, under the uniform scaling of the density $n_\lambda(\mathbf{r}) = \lambda^3 n(\lambda\mathbf{r})$, with $\lambda \geq 0$ ($\lambda = \alpha^{-1}$), the functionals have the following scaling behavior^{23,40}:

$$\begin{aligned} W_\infty[n_\lambda] &= \lambda W_\infty[n], \quad W_0[n_\lambda] = \lambda W_0[n], \\ W'_\infty[n_\lambda] &= \lambda^{3/2} W'_\infty[n], \quad W'_0[n_\lambda] = W'_0[n], \end{aligned} \quad (11)$$

such that

$$W_{xc,\alpha}^{UEG-ISI}[n_{\frac{1}{\alpha}}] = \alpha W_{xc,\alpha}^{UEG-ISI}[n]. \quad (12)$$

Note that all ISI-like functionals in the limit of $W'_0 \rightarrow -\infty$, can be written as

$$E_{xc}[n] = W_\infty + W'_\infty F(q), \quad (13)$$

$$W_\alpha[n] = W_\infty + (E_x - W_\infty)f(x), \quad (14)$$

with

$$q = \frac{E_x - W_\infty}{W'_\infty} > 0, \quad (15)$$

$$x = q\sqrt{\alpha}, \quad (16)$$

and $F(q) = \int_0^1 qf(\sqrt{\alpha}q)d\alpha$. The functions $F(q)$ and $f(x)$ for common ISI-like functionals are reported in the Appendix A. For the UEG-ISI we have

$$F^{UEG-ISI}(q) = \frac{2q(d+1)}{H(q) + 2d}, \quad (17)$$

$$f(x) = (d+1) \frac{H(x)^2 + 4dH(x) + 4}{H(2d + H(x))^2}, \quad (18)$$

$$H(x) = \sqrt{4 + (d+1)^2 x^2}. \quad (19)$$

For small q we have

$$F^{UEG-ISI}(q) \rightarrow q - \frac{q^3}{8}(d+1) + \mathcal{O}(q^5), \quad (20)$$

and thus

$$E_{xc}^{UEG-ISI}(q) \rightarrow E_x + W'_\infty \left(-\frac{q^3}{8}(d+1) + \mathcal{O}(q^5) \right). \quad (21)$$

For one electron systems, if W_∞ is computed exactly (which is the case for W_∞^{TPSS} and for the point-charge-plus-continuum (PC) model⁴⁰ for the hydrogen atom), we have that $q = 0$ and thus UEG-ISI is correctly one-electron self-correlation free. Actually for one electron systems, it should also be that $W'_\infty = 0$, which can only be the case for a meta-GGA functional like TPSS: in this case q is undefined, but still $W'_\infty q^n$ vanishes for any n , and thus the UEG-ISI correlation is zero. For other GGA models of W_∞ and W'_∞ see e.g. Refs.60 and 62 the genISI correlation of one electron systems is small but not exactly zero.

The only parameter of the UEG-ISI functional is d and it is fixed as described in section IV A

B. The genISI XC functional

To restore the α -term of the weak interaction limit expansion of Eq. (4) and to preserve the UEG limit constructed above, we consider the following expression for the genISI functional

$$W_{xc,\alpha}^{genISI}[n] = W_{xc,\alpha}^{UEG-ISI}[n] + \frac{a[n] p[n] \alpha}{(1 + r[n] p[n] \alpha)^3} \quad (22)$$

where

$$\begin{aligned} a[n] &= W_0 \left[1 + q^3 \frac{W'_\infty}{4W_0} (1+d) \right], \\ p[n] &= W'_0/W_0, \\ r[n] &= m \left(\frac{W_0}{W_\infty} \right)^3, \end{aligned} \quad (23)$$

and $m = 18.0$ was fixed by fitting to the correlation energy of the Hooke's atom with force constant $k = 1/4^{62,74}$. Considering the density scaling relations, we observe that

$$W_{xc,\alpha}^{genISI}[n_\alpha(\mathbf{r})] = \alpha W_{xc,\alpha}^{genISI}[n(\mathbf{r})]. \quad (24)$$

The genISI XC functional satisfies all the exact conditions also recovered by revISI⁴³ and LB⁴⁴ functionals, and additionally has an improved UEG limit.

The genISI XC energy is

$$\begin{aligned} E_{xc}^{genISI}[n] &= \int_0^1 d\alpha W_{xc,\alpha}^{genISI}[n] \\ &= E_{xc}^{UEG-ISI}[n] + E_{xc}^{add}[n] \end{aligned} \quad (25)$$

$$\text{with } E_{xc}^{add}[n] = \frac{a[n]p[n]}{2(r[n]p[n] + 1)^2}. \quad (26)$$

For small q and small E_c^{GL2} we have

$$\begin{aligned} E_{xc}^{add} &\rightarrow W'_\infty \left(\frac{q^3}{8}(d+1) + \mathcal{O}(q^5) \right) + \\ &+ \left(1 - \frac{m(d+1)W'_\infty(q^3 + \mathcal{O}(q^4))}{2W_\infty} \right) E_c^{GL2} + \mathcal{O}((E_c^{GL2})^2), \end{aligned} \quad (27)$$

which cancels the second term in Eq. (21), so that E_x is recovered for a larger range of q . Finally the total genISI XC energy behaves as

$$\begin{aligned} E_{xc}^{genISI} &\rightarrow E_x + W'_\infty \mathcal{O}(q^5) + \\ &+ \left(1 - \frac{m(d+1)W'_\infty(q^3 + \mathcal{O}(q^4))}{2W_\infty} \right) E_c^{GL2} + \mathcal{O}((E_c^{GL2})^2). \end{aligned} \quad (28)$$

For one electron systems $E_c^{GL2} = 0$ and thus genISI is one-electron self-correlation free, as discussed in section II B.

Finally, we recall that the genISI total energy is not size-consistent (as all other interpolation formula), but a simple size-consistent correction can be added to it⁵⁴.

III. COMPUTATIONAL DETAILS

All the calculations for jellium clusters and atoms have been performed with a modified version of the Engel code^{75,76}, using a radial numerical grid and Kohn-Sham LDA orbitals and densities. We consider 24 neutral jellium spheres with number of electrons $Z = 8, 18, 20, 34, 40, 58, 92, 132, 138, 186, 196, 254, 338, 398, 438, 440, 508, 556, 612, 638, 676, 758, 832$ and 912. We also consider all noble atoms from $Z = 2$ to 290 e^- .

Because the SCE and GL2 results are not available for such systems, we used some semilocal approximations of these quantities:

- W_{∞}^{TPSS} of Eq. (37) of Ref. 77 that is one the most accurate models for W_{∞} (see Tables I-III of Ref. 77 and Table I of Ref. 78);
- W_{∞}^{MGGA} of Eq. (D16) of Ref. 40 that is one the most accurate models for W'_{∞} (see table II of Ref. 40 and tables I and II of Ref. 79). We recall that the hPC GGA model for W'_{∞} is also very accurate⁶⁰;
- W_0^{TPSS} of Eq. (A1) of Ref. 80 that is one the most accurate models for GL2 correlation energy (see Table S12 of Ref. 63);
- $W_0 = E_x$ the exact exchange computed with LDA orbitals.

We note that for jellium clusters and large atoms, the meta-GGA approximations of W_{∞} , W'_{∞} , and W_0 are expected to be accurate, such that their use in ISI-like functionals should give realistic results.

IV. RESULTS

A. UEG correlation energy

The XC energy $E_{xc} = \int d\mathbf{r} n(\mathbf{r})\epsilon_{xc}(\mathbf{r})$ is just $E_{xc} = N\epsilon_{xc}(r_s)$ in case of the spin-unpolarized UEG, where N is the number of electrons and $\epsilon_{xc}(r_s)$ is the XC energy per particle. We also note that $W_0 = N(-3/(4\pi))k_F$, $W_{\infty} = An^{1/3}N$, $W'_{\infty} = Bn^{1/2}N$, where $k_F = (3\pi^2n)^{1/3}$, $n = 3/[4\pi r_s^3]$, $A = -1.451$ and $B = 1.535$. Thus $q = 0.4641n^{-1/6}$. Substituting these expressions in the UEG limit of ISI-like functionals, we obtain their correlation energies per particle $\epsilon_c(r_s)$. In the Appendix A, we show the expressions of ISI, revISI, SPL⁴², and LB⁸¹ XC functionals and their UEG limits.

The parameter d of the UEG-ISI functional was found by minimizing the expression

$$Error(d) = \int_1^{10} d r_s |\epsilon_c^{UEG-ISI}(d, r_s) - \epsilon_c^{exact}(r_s)|, \quad (29)$$

and the results are reported in Fig. 1. At $d \approx 0$ and $d \approx 0.74$, the $Error(0) \approx 0.138$ and $Error(0.74) \approx 0.08$ are similar with the ones given by ISI and revISI, respectively. The curve $Error(d)$ has only one minimum at $d = 3.5$ where $Error(3.5) \approx 0.003$.

In Fig. 2 we show our UEG results. Both SPL and LB functionals behave similarly as $\epsilon_c = -0.44196/r_s$, being accurate only in the low-density limit. On the other hand, the ISI functional is definitely better and in the high-density limit, behaves as

$$\epsilon_c^{ISI} \rightarrow -0.1736/\sqrt{r_s}, \quad \text{when } r_s \rightarrow 0. \quad (30)$$

Moreover, the revISI shows a quite good improvement over the ISI functional, behaving as

$$\epsilon_c^{revISI} \rightarrow -0.130/\sqrt{r_s}, \quad \text{when } r_s \rightarrow 0. \quad (31)$$

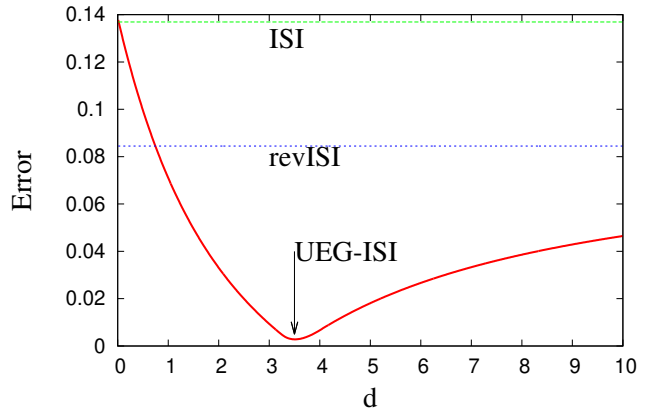


FIG. 1. $Error = \int_1^{10} d r_s |\epsilon_c^{approx}(d, r_s) - \epsilon_c^{exact}(r_s)|$ versus the parameter d . Also shown are the errors from ISI and revISI functionals.

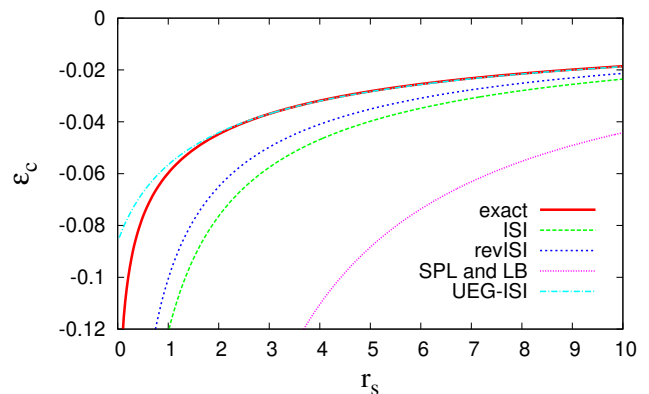


FIG. 2. UEG correlation energy per particle $\epsilon_c(r_s)$ versus the bulk parameter r_s , from several ISI-like functionals. The exact curve is the accurate parametrization of the Perdew and Wang⁶.

However, the UEG-ISI functional shows the best performance, being almost exact for $r_s \geq 1$, while in the high-density limit is just a constant

$$\epsilon_c^{UEG-ISI} \rightarrow -0.0192(1+d) = -0.086, \quad \text{when } r_s \rightarrow 0. \quad (32)$$

We recall that $\epsilon_c^{exact} \rightarrow 0.031091 \ln(r_s) - 0.0469203$ for spin-unpolarized case⁶ when $r_s \rightarrow 0$, such that the exchange energy per particle $\epsilon_x \rightarrow -0.4582/r_s$ is dominating. We note also that the constant term in the exact high-density limit expansion is almost twice smaller than the one from UEG-ISI limit.

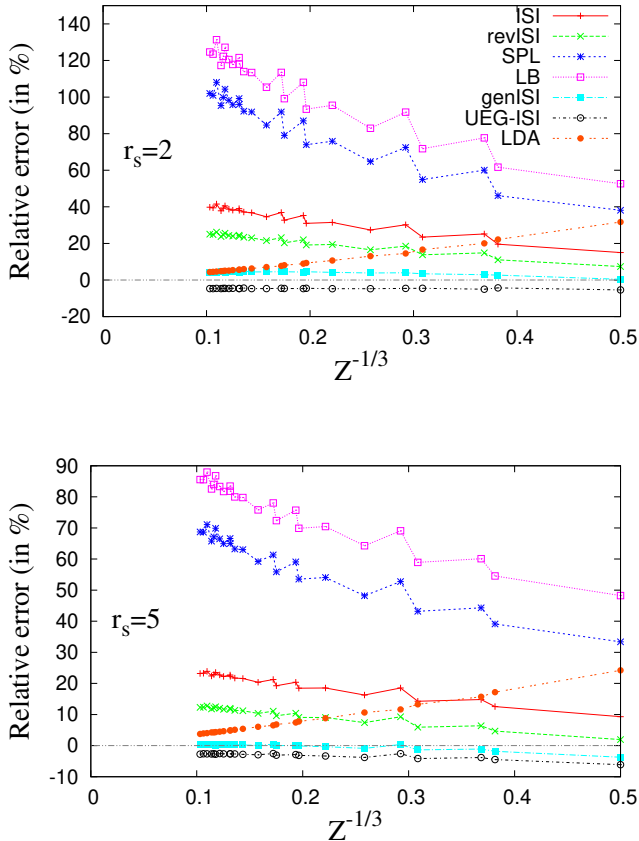


FIG. 3. Relative error $[(\text{approx} - \text{reference}) / \text{reference}] \times 100$ of the correlation energy of jellium clusters (from $Z = 8$ to $912 e^-$) versus $Z^{-1/3}$, for $r_s = 2$ (upper panel) and $r_s = 5$ (lower panel). For the reference correlation energy, we use the TPSS one, which is very accurate for such systems⁸².

B. Jellium clusters

We present in Fig. 3 the correlation energy relative errors (RE) of the considered jellium clusters for $r_s = 2$ (upper panel) and $r_s = 5$ (lower panel), respectively. The ISI-like methods have a similar trend as in the UEG case (see Fig. 1). revISI gives a good improvement over the ISI functional, but in both cases, the errors increase with Z . Contrary to this trend, the LDA error decreases with Z . However, the best performances are reported from the genISI (with $0.3\% \leq \text{RE} \leq 4.8\%$ for the upper panel, and $-4\% \leq \text{RE} \leq 0.5\%$ for the lower panel) and the UEG-ISI (with $-3.8\% \leq \text{RE} \leq -2.8\%$ for the upper panel, and $-5.6\% \leq \text{RE} \leq -2.2\%$ for the lower panel).

We summarize our results in Table I, where we present the MAREs in correlation energy of the considered XC functionals, for several values of bulk parameters. We observe that all functionals show a worsening of their prediction when r_s decreases. However, both genISI and UEG-ISI are remarkably accurate, with $\text{MARE} \leq 5\%$.

TABLE I. Mean absolute relative error (MARE in %) of correlation energy from 24 jellium clusters ($8 \leq Z \leq 912$), for several bulk parameters. The best results have been highlighted in boldface. We use the TPSS correlation as the reference correlation energy, because it predicts with high accuracy the diffusion Monte Carlo (DMC) results corrected for the fixed-node DMC error (see tables VI and VII of Ref. 82). To our best knowledge, there are not high-level, benchmark results available for jellium clusters with $Z > 106$.

r_s	2	3	4	5
ISI	33.7	27.0	22.8	19.9
revISI	20.9	15.5	12.2	10.0
SPL	83.9	72.4	64.4	58.5
LB	104.4	91.4	82.1	75.0
UEG-ISI	4.7	3.8	3.4	3.1
genISI	4.0	1.8	0.9	0.6
LDA	9.7	8.7	8.2	7.9

Finally, let us consider the jellium sphere with $Z = 912$ and $r_s = 4$. In the upper panel of Fig. 4, we show the reduced density gradients $s(\mathbf{r})$ and $q(\mathbf{r})$ inside of this sphere. Note that q in this paragraph is the reduced Laplacian and not the global parameter in Eq. 15. We observe that both s and q are very small ($s \leq 0.1$, $-0.1 \leq q \leq 0.05$), showing the shell structure oscillations, and only near the boundary of the cluster, when the density starts to decay, the reduced gradients become large. Thus, the core of this sphere is a typical example of a slowly varying density, a difficult case for the ISI-like functionals. In the lower panel of Fig. 4, we report the coupling constant correlation integrand $W_{c,\alpha} = W_{xc,\alpha} - W_0$, for $0 \leq \alpha \leq 1$. The area under each curve is the correlation energy. We observe that genISI has the same correct behavior at $\alpha \rightarrow 0$ as ISI and revISI (see Eq. (4)), while for $\alpha \geq 0.3$, it smoothly recovers the UEG-ISI functional.

C. Noble atoms

In the upper panel of Fig. 5, we report the ratio $p[n] = W'_0/W_0$ of the noble atoms (from $Z = 2$ to $290 e^-$). One can note that it is very small, decreasing from 0.094 (He atom) to 0.018 ($290 e^-$ atom), in an almost linear pattern that predicts $p[n] \rightarrow 0$ in the limit $Z \rightarrow \infty$. Thus, the core of large atoms is a typical example of a high-density system where the exchange energy dominates over the GL2 correlation energy.

In the lower panel of Fig. 5, we report the relative errors of the correlation energy for these systems. All ISI-like functionals are quite accurate, within a maximum error of $\pm 10\%$. Note that genISI and revISI give similar results, showing the best performances. In this case, the UEG-ISI functional, not shown in the figure, fail badly, with relative errors $-60\% \leq \text{RE} \leq 80\%$.

In order to understand better the behavior of genISI for large atoms, we investigate in more detail the case of

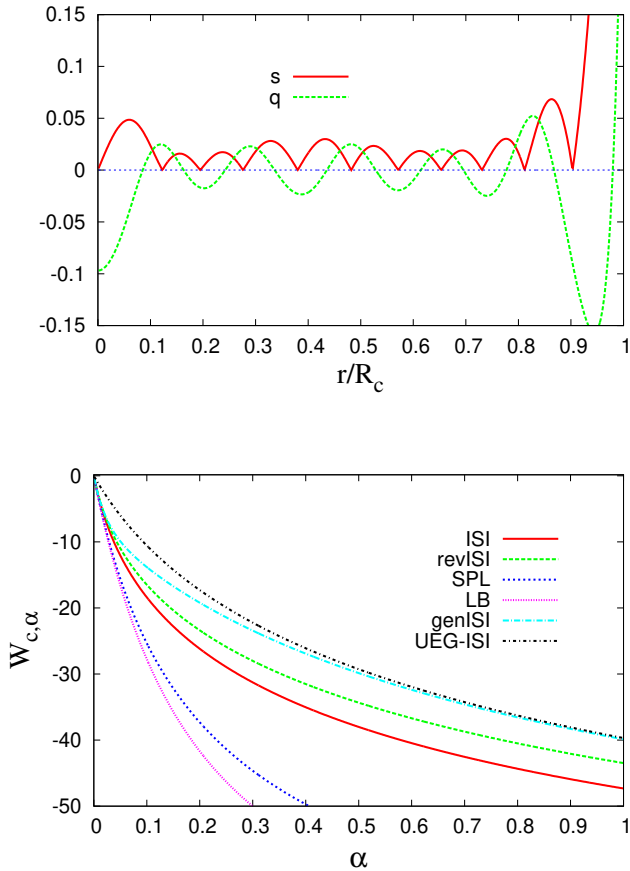


FIG. 4. Upper panel: The reduced gradient $s = |\nabla n|/[2k_F n]$ and the reduced Laplacian $q = \nabla^2 n/[4k_F^2 n]$, versus the normalized radial distance r/R_c , for the jellium sphere with $Z = 912$ and $r_s = 4$. Here $R_c = r_s Z^{1/3} \approx 38.79$ a.u. is the radius of the sphere.

Lower panel: The adiabatic connection correlation integrand $W_{c,\alpha} = W_{xc,\alpha} - W_0$ versus α for the same jellium cluster ($Z = 912$ and $r_s = 4$). The area under each curve is the correlation energy: $E_c^{ISI} = -34.856$ Ha, $E_c^{revISI} = -31.605$ Ha, $E_c^{genISI} = -27.759$ Ha, $E_c^{UEG-ISI} = -26.689$ Ha, and $E_c^{TPSS} = -27.525$ Ha.

the noble atom with $Z = 290$. In the upper panel of Fig. 6, we show that s and q are small inside the atomic core, with the exception of nucleus region where $q \rightarrow -\infty$ and $s \approx 0.4$, due to the cusp of the density at the nucleus. However, at the nucleus, $r_s \approx 0.0024$ is very small, such that this region approaches the high-density limit.

In the lower panel of Fig. 6, we report the coupling constant correlation integrand $W_{c,\alpha}$, for $0 \leq \alpha \leq 1$, such that the area under each curve is the correlation energy. We observe that $W_{c,\alpha}^{genISI}$ and $W_{c,\alpha}^{revISI}$ are almost indistinguishable. Now, the UEG-ISI is very different from genISI, and only at large coupling constants ($\alpha \geq 50$) both functionals will start to agree (as shown in the inset of the lower panel of Fig. 6).

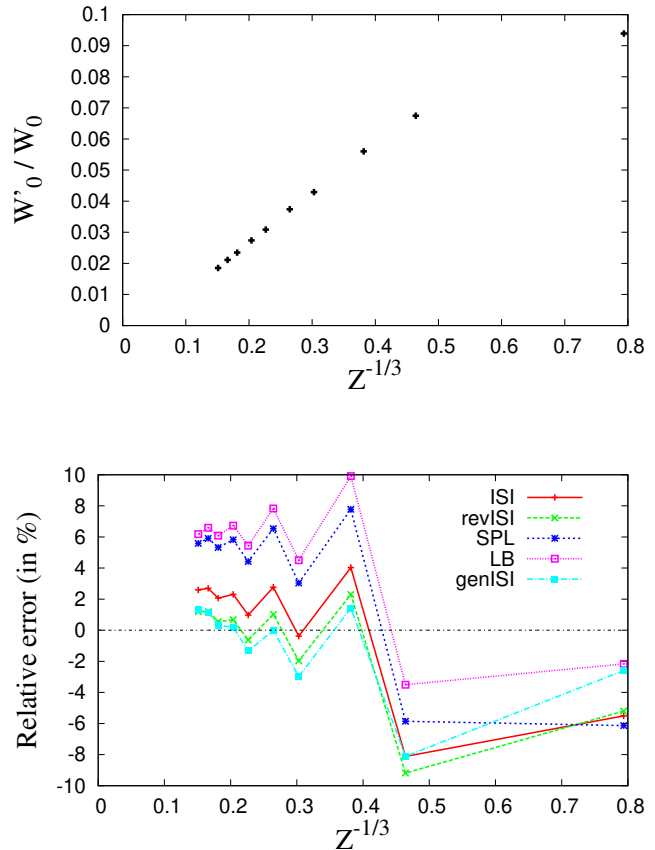


FIG. 5. Upper panel: The ratio $p[n] = W'_0/W_0$ of noble atoms (from $Z = 2$ to $290 e^-$) versus $Z^{-1/3}$.

Lower panel: Relative error $[(approx - reference)/reference] \times 100$ of the correlation energy of noble atoms (from $Z = 2$ to $290 e^-$) versus $Z^{-1/3}$. The reference correlation energy is: for $Z \leq 86$ (a.i. until Rn atom) we use the benchmark data shown in Tables I and II of Ref. 83 (that was taken from Refs.⁸⁴⁻⁸⁶), and for the atoms with $118 \leq Z \leq 290$ we use the acGGA correlation functional of Ref. 87, that was built from semiclassical atom theory, being very accurate for large atoms.

D. Small systems with exact ingredients (W_0 , W'_0 , W_∞^{SCE} , and W'_∞^{SCE})

As a final part of this section, in Table II, we show the correlation energies for several ISI-like expressions for two model systems and a few small atoms, using very accurate low- and high-density expansion ingredients (W_0 , W'_0 , W_∞ , and W'_∞). In the last column, we report the MARE for each method. The inspection of the table reveals that ISI, revISI and genISI have almost the same accuracy with a MARE in the range 4.0%-4.6%. The SPL and LB expressions provide errors, which are about 2% worse than ISI. The worst performance is given by the UEG-ISI formula, which yields MARE of 61.1%. This is not surprising since this model was designed to be accu-

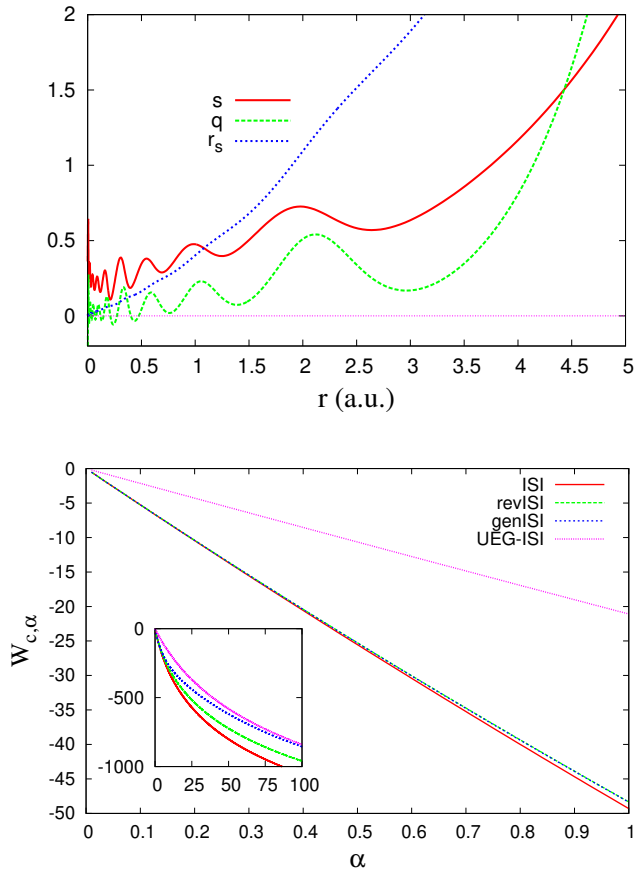


FIG. 6. Upper panel: The bulk parameter $r_s(r)$ and the reduced gradients $s(r)$ and $q(r)$, versus the radial distance from the nucleus r , for the noble atom with $Z = 290$. Lower panel: The adiabatic connection correlation integrand $W_{c,\alpha}$ versus α ($0 \leq \alpha \leq 1$) for the noble atom with $Z = 290$. The area under each curve is the correlation energy: $E_c^{ISI} = -25.240$ Ha, $E_c^{revISI} = -24.895$ Ha, $E_c^{genISI} = -24.924$ Ha, $E_c^{UEG-ISI} = -10.613$ Ha, and $E_c^{ref} = -24.602$ Ha. The inset shows $W_{c,\alpha}$ versus α , for $\alpha \leq 100$.

rate in the UEG limit where $W'_0 \rightarrow -\infty$, and it shows the importance of the E_{xc}^{add} term.

We also note that the same trend shown in Table II was also reported for the correlation energies of noble atoms with $2 \leq Z \leq 290$ (see the lower panel of Fig. 5), even if they were computed with meta-GGA approximations for W'_0 , W_∞ , and W'_∞ .

V. CONCLUSIONS

We have constructed the UEG-ISI XC functional, which depends on $W_0[n]$, $W_\infty[n]$ and $W'_\infty[n]$, being remarkably accurate for the UEG model system. The UEG-ISI XC functional behaves correctly in the strong-interaction limit, while in the weak-interaction limit it recovers only the leading term $W_0[n]$. We have also de-

TABLE II. The correlations energies for several ISI-like expressions computed for Hooke's atom with force constant $\omega = 0.5$, two-electron exponential density (Exp) with $n(r) = 2 \exp(-2r)/\pi$, and He, Be, and Ne atoms using the exact ingredients (W_0 , W'_0 , W_∞^{SCE} , and W'_∞^{SCE}). All reference data have been taken from Table I of Ref. 62 and the references therein. In the last column, we report the MARE (in %) for a given method.

	Hook	Exp.	He	Be	Ne	
W_∞^{SCE}	-0.743	-0.910	-1.500	-4.020	-20.000	
W'_∞^{SCE}	0.208	0.308 ^{a)}	0.621	2.590	22.000	
W_0	-0.515	-0.625	-1.025	-2.674	-12.084	
W'_0	-0.101	-0.093	-0.101	-0.250	-0.938	
						MARE (%)
SPL	-0.036	-0.035	-0.042	-0.106	-0.420	6.0
LB	-0.038	-0.037	-0.044	-0.110	-0.432	6.3
ISI	-0.037	-0.036	-0.043	-0.104	-0.410	4.6
revISI	-0.037	-0.036	-0.043	-0.104	-0.405	4.0
UEG-ISI	-0.061	-0.064	-0.086	-0.144	-0.474	61.1
genISI	-0.040	-0.038	-0.043	-0.108	-0.411	4.5
Exact	-0.039	-0.037	-0.042	-0.096	-0.394	

a) - computed using hPC model from Ref.60

veloped the genISI XC functional, by adding a GL2 correction to the UEG-ISI, such that the genISI fulfills all the known exact requirements, and additionally it is accurate for the UEG, especially in the region $1 \leq r_s \leq 10$, that is the most relevant in solid-state applications.

The genISI and UEG-ISI have been tested for the correlation energies of 24 neutral jellium spheres with number of electrons $8 \leq Z \leq 912$. The $W_{xc,\alpha}^{genISI}$ and $W_{xc,\alpha}^{UEG-ISI}$ are similar, with the exception of $\alpha \rightarrow 0$ region, where $W_{xc,\alpha}^{genISI}$ recovers the first two terms of the GL perturbation expansion of Eq. (4). Consequently, both genISI and UEG-ISI give very good and almost similar performances for jellium clusters, as reported in Table I and Fig. 3.

We have also tested the genISI and UEG-ISI functionals for noble atoms with $2 \leq Z \leq 290$, where the ratio $p[n]$ is small ($p[n] \leq 0.1$), such that genISI and UEG-ISI behave differently. Thus while the genISI is quite accurate with a relative error below 7% (see Fig. 5 (lower panel)), the UEG-ISI fails badly, with errors larger than 40%, as shown in Fig. 6 (lower panel). This fact shows that the genISI correction to the UEG-ISI plays a vital role in this functional construction.

Finally, we have also presented the results from few small systems where the ingredients W_0 , W'_0 , W_∞^{SCE} , and W'_∞^{SCE} are known with high accuracy. The genISI shows a reasonable performance, in line with the other ISI-like methods.

Application of genISI to molecular systems is straightforward, with the methods and limitations previously discussed in Refs. 52, 54, 60, 63, and 67. We expect that the method of genISI development can be further used for the construction of more accurate ISI-like functionals, towards their use in solid-state and material science

calculations.

ACKNOWLEDGMENTS

L.A.C. and F.D.S. acknowledge the financial support from ICSC - Centro Nazionale di Ricerca in High Performance Computing, Big Data and Quantum Computing, funded by European Union - NextGenerationEU - PNRR. F.D.S acknowledges the financial support from PRIN project no. 2022LM2K5X, Adiabatic Connection for Correlation in Crystals (AC^3). S.Ś. thanks to the Polish National Science Center for the partial financial support under Grant No. 2020/37/B/ST4/02713.

Appendix A: ISI-like methods

1. Interaction Strength Interpolation (ISI) functional³⁹

$$W_\alpha^{ISI} = W_\infty + \frac{X}{\sqrt{1 + \alpha Y + Z}} \quad (\text{A1})$$

$$E_{xc}^{ISI} = W_\infty + \frac{2X}{Y} \left[\sqrt{1 + Y} - 1 - Z \ln \left(\frac{\sqrt{1 + Y} + Z}{1 + Z} \right) \right] \quad (\text{A2})$$

with

$$X = \frac{xy^2}{z^2}, Y = \frac{x^2y^2}{z^4}, Z = \frac{xy^2}{z^3} - 1 \quad (\text{A3})$$

$$x = -4E_c^{GL2}, y = W'_\infty, z = E_x - W_\infty \quad (\text{A4})$$

$$F^{ISI}(q) = 2 - 2 \frac{\ln(1+q)}{q} \quad (\text{A5})$$

$$f^{ISI}(x) = \frac{1}{1+x} \quad (\text{A6})$$

2. Revised ISI (revISI) functional⁴³

$$W_\alpha^{revISI} = W_\infty + \frac{b(2 + c\alpha + 2d\sqrt{1 + c\alpha})}{2\sqrt{1 + c\alpha}(d + \sqrt{1 + c\alpha})^2} \quad (\text{A7})$$

$$E_{xc}^{revISI} = W_\infty + \frac{b}{\sqrt{1 + c + d}} \quad (\text{A8})$$

with

$$b = -\frac{8E_c^{GL2}(W'_\infty)^2}{(E_x - W_\infty)^2} \quad (\text{A9})$$

$$c = \frac{16(E_c^{GL2}W'_\infty)^2}{(E_x - W_\infty)^4} \quad (\text{A10})$$

$$d = -1 - \frac{8E_c^{GL2}(W'_\infty)^2}{(E_x - W_\infty)^3} \quad (\text{A11})$$

Now, putting values of b, c , and d in Eq.(B7) we get

$$E_{xc}^{revISI} = W_\infty + \frac{8E_c^{GL2}(W'_\infty)^2}{(W_0 - W_\infty)^2 \left(1 + \frac{8E_c^{GL2}(W'_\infty)^2}{(W_0 - W_\infty)^2} - \sqrt{1 + \frac{16(E_c^{GL2}W'_\infty)^2}{(W_0 - W_\infty)^4}} \right)} \quad (\text{A12})$$

$$F^{revISI}(q) = \frac{2q}{q+2} \quad (\text{A13})$$

$$f^{revISI}(x) = \frac{4+x}{x^2+4x+4} \quad (\text{A14})$$

3. Seidl-Perdew-Levy (SPL) functional⁴²

$$W_\alpha^{SPL} = W_\infty + \frac{W_0 - W_\infty}{\sqrt{1 + 2\alpha\chi}} \quad (\text{A15})$$

$$E_{xc}^{SPL} = E_x + (E_x - W_\infty) \left[\frac{\sqrt{1 + 2\chi} - 1 - \chi}{\chi} \right] \quad (\text{A16})$$

with

$$\chi = \frac{2E_c^{GL2}}{W_\infty - E_x} \quad (\text{A17})$$

$$F^{SPL}(q) = f^{SPL}(x) = 0 \quad (\text{A18})$$

4. Liu-Burke (LB) functional⁴⁴

$$W_\alpha^{LB} = W_\infty + b(y + y^4) \quad (\text{A19})$$

$$E_{xc}^{LB} = E_x + \frac{2b}{c} \left[\sqrt{1 + c} - \frac{1 + c/2}{1 + c} - c \right] \quad (\text{A20})$$

with

$$y = \frac{1}{\sqrt{1 + c\alpha}}, b = \frac{E_x - W_\infty}{2}, c = \frac{8E_c^{GL2}}{5(W_\infty - E_x)} \quad (\text{A21})$$

$$F^{LB}(q) = f^{LB}(x) = 0 \quad (\text{A22})$$

-
- ¹ P. Hohenberg and W. Kohn, Phys. Rev. **136**, B864 (1964).
- ² W. Kohn and L. J. Sham, Phys. Rev. **140**, A1133 (1965).
- ³ J. P. Perdew and K. Schmidt, in *AIP Conference Proceedings* (IOP INSTITUTE OF PHYSICS PUBLISHING LTD, 2001) pp. 1–20.
- ⁴ J. P. Perdew, A. Ruzsinszky, J. Tao, V. N. Staroverov, G. E. Scuseria, and G. I. Csonka, J. Chem. Phys. **123**, 062201 (2005).
- ⁵ P. A. Dirac, in *Mathematical Proceedings of the Cambridge Philosophical Society*, Vol. 26 (Cambridge University Press, 1930) pp. 376–385.
- ⁶ J. P. Perdew and Y. Wang, Phys. Rev. B **45**, 13244 (1992).
- ⁷ P.-F. Loos and P. M. W. Gill, WIREs Computational Molecular Science **6**, 410–429 (2016).
- ⁸ A. Patra, S. Jana, L. A. Constantin, L. Chiodo, and P. Samal, J. Chem. Phys. **152**, 151101 (2020).
- ⁹ A. Patra, J. E. Bates, J. Sun, and J. P. Perdew, Proceedings of the National Academy of Sciences, 201713320 (2017).
- ¹⁰ N. E. Singh-Miller and N. Marzari, Phys. Rev. B **80**, 235407 (2009).
- ¹¹ D. C. Langreth and J. P. Perdew, Solid State Communications **17**, 1425 (1975).
- ¹² O. Gunnarsson and B. I. Lundqvist, Phys. Rev. B **13**, 4274 (1976).
- ¹³ A. Savin, F. Colonna, and R. Pollet, Int. J. Quantum Chem. **93**, 166 (2003).
- ¹⁴ A. J. Cohen, P. Mori-Sánchez, and W. Yang, J. Chem. Phys. **127**, 034101 (2007).
- ¹⁵ M. Ernzerhof, Chem. Phys. Lett. **263**, 499 (1996).
- ¹⁶ K. Burke, M. Ernzerhof, and J. P. Perdew, Chem. Phys. Lett. **265**, 115 (1997).
- ¹⁷ F. Colonna and A. Savin, J. Chem. Phys. **110**, 2828 (1999).
- ¹⁸ W. Kohn, A. D. Becke, and R. G. Parr, J. Phys. Chem. **100**, 12974 (1996).
- ¹⁹ A. D. Becke, J. Chem. Phys. **98**, 5648 (1993).
- ²⁰ C. Adamo and V. Barone, J. Chem. Phys. **108**, 664 (1998).
- ²¹ S. Śmiga and L. A. Constantin, J. Phys. Chem. A **124**, 5606 (2020).
- ²² A. Görling and M. Levy, Phys. Rev. A **50**, 196 (1994).
- ²³ A. Görling and M. Levy, Phys. Rev. B **47**, 13105 (1993).
- ²⁴ A. Görling and M. Levy, Phys. Rev. A **52**, 4493 (1995).
- ²⁵ J. F. Dobson, J. Wang, and T. Gould, Phys. Rev. B **66**, 081108 (2002).
- ²⁶ A. V. Terentjev, L. A. Constantin, and J. M. Pitarke, Phys. Rev. B **98**, 085123 (2018).
- ²⁷ L. A. Constantin, Phys. Rev. B **93**, 121104 (2016).
- ²⁸ M. Corradini, R. Del Sole, G. Onida, and M. Palumbo, Phys. Rev. B **57**, 14569 (1998).
- ²⁹ J. Toulouse, Phys. Rev. B **72**, 035117 (2005).
- ³⁰ C. F. Richardson and N. W. Ashcroft, Phys. Rev. B **50**, 8170 (1994).
- ³¹ J. E. Bates, S. Laricchia, and A. Ruzsinszky, Phys. Rev. B **93**, 045119 (2016).
- ³² J. E. Bates, J. Sensenig, and A. Ruzsinszky, Phys. Rev. B **95**, 195158 (2017).
- ³³ A. Ruzsinszky, L. A. Constantin, and J. M. Pitarke, Phys. Rev. B **94**, 165155 (2016).
- ³⁴ J. F. Dobson and J. Wang, Phys. Rev. B **62**, 10038 (2000).
- ³⁵ A. Görling, Int. J. Quantum Chem. **69**, 265 (1998).
- ³⁶ Y.-H. Kim and A. Görling, Phys. Rev. Lett. **89**, 096402 (2002).
- ³⁷ J. Erhard, P. Bleiziffer, and A. Görling, Phys. Rev. Lett. **117**, 143002 (2016).
- ³⁸ C. E. Patrick and K. S. Thygesen, J. Chem. Phys. **143**, 102802 (2015).
- ³⁹ M. Seidl, J. P. Perdew, and S. Kurth, Phys. Rev. Lett. **84**, 5070 (2000).
- ⁴⁰ M. Seidl, J. P. Perdew, and S. Kurth, Phys. Rev. A **62**, 012502 (2000).
- ⁴¹ J. P. Perdew, S. Kurth, and M. Seidl, Int. J. Mod. Phys. B **15**, 1672 (2001).
- ⁴² M. Seidl, J. P. Perdew, and M. Levy, Phys. Rev. A **59**, 51 (1999).
- ⁴³ P. Gori-Giorgi, G. Vignale, and M. Seidl, J. Chem. Theory Comput. **5**, 743 (2009).
- ⁴⁴ Z.-F. Liu and K. Burke, Phys. Rev. A **79**, 064503 (2009).
- ⁴⁵ Z.-F. Liu and K. Burke, J. Chem. Phys. **131**, 124124 (2009).
- ⁴⁶ R. Magyar, W. Terilla, and K. Burke, J. Chem. Phys. **119**, 696 (2003).
- ⁴⁷ J. Sun, J. Chem. Theory Comput. **5**, 708 (2009).
- ⁴⁸ M. Seidl and P. Gori-Giorgi, Phys. Rev. A **81**, 012508 (2010).
- ⁴⁹ A. Mirschink, M. Seidl, and P. Gori-Giorgi, J. Chem. Theory Comput. **8**, 3097 (2012).
- ⁵⁰ P. Gori-Giorgi and M. Seidl, Phys. Chem. Chem. Phys. **12**, 14405 (2010).
- ⁵¹ S. Vuckovic, T. J. Irons, A. Savin, A. M. Teale, and P. Gori-Giorgi, J. Chem. Theory Comput. **12**, 2598 (2016).
- ⁵² E. Fabiano, P. Gori-Giorgi, M. Seidl, and F. Della Sala, J. Chem. Theory Comput. **12**, 4885 (2016).
- ⁵³ S. Giarrusso, P. Gori-Giorgi, F. Della Sala, and E. Fabiano, J. Chem. Phys. **148**, 134106 (2018).
- ⁵⁴ S. Vuckovic, P. Gori-Giorgi, F. Della Sala, and E. Fabiano, J. Phys. Chem. Lett. (2018).
- ⁵⁵ D. P. Kooi and P. Gori-Giorgi, Theor. Chem. Acc. **137**, 166 (2018).
- ⁵⁶ Y. Zhou, H. Bahmann, and M. Ernzerhof, J. Chem. Phys. **143**, 124103 (2015).
- ⁵⁷ M. Seidl, S. Giarrusso, S. Vuckovic, E. Fabiano, and P. Gori-Giorgi, J. Chem. Phys. **149**, 241101 (2018).
- ⁵⁸ S. Vuckovic, A. Gerolin, T. J. Daas, H. Bahmann, G. Friesecke, and P. Gori-Giorgi, Wiley Interdisciplinary Reviews: Computational Molecular Science **13**, e1634 (2023).
- ⁵⁹ E. Fabiano, S. Śmiga, S. Giarrusso, T. J. Daas, F. Della Sala, I. Grabowski, and P. Gori-Giorgi, J. Chem. Theory Comput. **15**, 1006 (2019).
- ⁶⁰ S. Śmiga, F. Della Sala, P. Gori-Giorgi, and E. Fabiano, J. Chem. Theory Comput. **18**, 5936 (2022).
- ⁶¹ T. J. Daas, E. Fabiano, F. Della Sala, P. Gori-Giorgi, and S. Vuckovic, J. Phys. Chem. Letters **12**, 4867 (2021).
- ⁶² L. A. Constantin, Phys. Rev. B **99**, 085117 (2019).
- ⁶³ S. Śmiga and L. A. Constantin, J. Chem. Theory Comput. **16**, 4983 (2020).
- ⁶⁴ S. Vuckovic, T. J. Irons, L. O. Wagner, A. M. Teale, and P. Gori-Giorgi, Phys. Chem. Chem. Phys. **19**, 6169 (2017).
- ⁶⁵ S. Vuckovic and P. Gori-Giorgi, J. Phys. Chem. Lett. **8**, 2799 (2017).

- ⁶⁶ T. J. Daas, D. P. Kooi, T. Benyahia, M. Seidl, and P. Gori-Giorgi, arXiv preprint arXiv:2211.07512 (2022).
- ⁶⁷ Y. J. Franzke, C. Holzer, J. H. Andersen, T. Begušić, F. Bruder, S. Coriani, F. Della Sala, E. Fabiano, D. A. Fedotov, S. Fürst, S. Gillhuber, R. Grotjahn, M. Kaupp, M. Kehry, M. Krstić, F. Mack, S. Majumdar, B. D. Nguyen, S. M. Parker, F. Pauly, A. Pausch, E. Perlt, G. S. Phun, A. Rajabi, D. Rappoport, B. Samal, T. Schrader, M. Sharma, E. Tapavicza, R. S. Treß, V. Voora, A. Wodyński, J. M. Yu, B. Zerulla, F. Furche, C. Hättig, M. Sierka, D. P. Tew, and F. Weigend, *J. Chem. Theory Comput.* **0**, null (0).
- ⁶⁸ S. Jana, S. Śmiga, L. A. Constantin, and P. Samal, *J. Chem. Theory Comput.* **16**, 7413 (2020).
- ⁶⁹ P. Gori-Giorgi, M. Seidl, and G. Vignale, *Phys. Rev. Lett.* **103**, 166402 (2009).
- ⁷⁰ F. Malet and P. Gori-Giorgi, *Phys. Rev. Lett.* **109**, 246402 (2012).
- ⁷¹ G. Friesecke, A. Gerolin, and P. Gori-Giorgi, arXiv preprint arXiv:2202.09760 (2022).
- ⁷² L. Goerigk and S. Grimme, *Wiley Interdisciplinary Reviews: Computational Molecular Science* **4**, 576 (2014).
- ⁷³ B. P. Harding, Z. Mauri, and A. Pribram-Jones, *J. Chem. Phys.* **156** (2022).
- ⁷⁴ M. Taut, *Journal of Physics A: Mathematical and General* **27**, 1045 (1994).
- ⁷⁵ E. Engel and S. H. Vosko, *Phys. Rev. A* **47**, 2800 (1993).
- ⁷⁶ E. Engel, in *A primer in density functional theory* (Springer, 2003) pp. 56–122.
- ⁷⁷ J. P. Perdew, J. Tao, V. N. Staroverov, and G. E. Scuseria, *J. Chem. Phys.* **120**, 6898 (2004).
- ⁷⁸ S. Jana, S. Śmiga, L. A. Constantin, and P. Samal, “Semilocal Meta-GGA Exchange-Correlation Approximation From Adiabatic Connection Formalism: Extent and Limitations,” (2023), arXiv:2212.04610 [cond-mat].
- ⁷⁹ S. Jana, S. Śmiga, L. A. Constantin, and P. Samal, arXiv preprint arXiv:2212.04610 (2022).
- ⁸⁰ J. P. Perdew, V. N. Staroverov, J. Tao, and G. E. Scuseria, *Phys. Rev. A* **78**, 052513 (2008).
- ⁸¹ Z.-F. Liu and K. Burke, *Phys. Rev. A* **79**, 064503 (2009).
- ⁸² J. Tao, J. P. Perdew, L. M. Almeida, C. Fiolhais, and S. Kümmel, *Phys. Rev. B* **77**, 245107 (2008).
- ⁸³ K. Burke, A. Cancio, T. Gould, and S. Pittalis, *J. Chem. Phys.* **145**, 054112 (2016).
- ⁸⁴ S. P. McCarthy and A. J. Thakkar, *J. Chem. Phys.* **134**, 044102 (2011).
- ⁸⁵ S. P. McCarthy and A. J. Thakkar, *J. Chem. Phys.* **136** (2012).
- ⁸⁶ S. J. Chakravorty, S. R. Gwaltney, E. R. Davidson, F. A. Parpia, and C. F. Fischer, *Phys. Rev. A* **47**, 3649 (1993).
- ⁸⁷ K. Burke, A. Cancio, T. Gould, and S. Pittalis, arXiv preprint arXiv:1409.4834 (2014).